Numerical Modeling and Performance Evaluation of SnS Based Heterojunction Solar Cell with p^+ SnS BSF Layer

Payel Bhattacharjee
KIIT University School of Electronics Engineering
Rajeshwari Garain
KIIT University School of Electronics Engineering
Arindam Basak (arindambasak2007@gmail.com)
KIIT https://orcid.org/0000-0003-3943-4415
Udai P. Singh
KIIT University School of Electronics Engineering

Research Article

Keywords: Simulation, SnS solar cell, BSF layer, Optimization

Posted Date: March 11th, 2022

DOI: https://doi.org/10.21203/rs.3.rs-1114157/v1

Abstract

In this research article, the performance of the solar cell having the structure (Ag/ZnO:Al/CdS/SnS/p^+-SnS/Mo/Glass) is investigated in detail using SCAPS-1D software. The main motive of this work was to study the performance parameters of SnS based solar cell having p^+-SnS layer as Back Surface Field (BSF). It is found that with the addition of p^+-SnS BSF layer and after performing all the optimization of the different parameters, the efficiency (η) of the solar cell improved and enhanced to 7.11%. The open circuit voltage (V_{oc}) and the short circuit current (J_{sc}) of the designed solar cell enhanced up to 359 mV and 27 mA/cm^2 after adding p^+-SnS BSF layer. It is observed that the performance of the heterojunction solar cell is dependent on several factors like thickness of the buffer, absorber and the BSF layer, carrier concentration, defect density, series and shunt resistance of the device. Also fabricating a p^+-SnS layer is of low cost and the lattice mismatch is less with the SnS layer. All these findings reveal that p^+-SnS layer could be a promising BSF layer to enhance the performance of SnS based heterojunction solar cell.

Introduction

In recent days, thinfilm solar cell is getting utmost interest among the research community. However, with this dynamic market scenario, developing a commercially viable thin film solar cell is a challenge. Different types of solar cells and solar cell materials are available in the market to develop thin film based solar cells [1]. SnS, a IV-VI semiconductor, based thin film solar cell is one of the most promising type of solar cell due to the direct bandgap (1.3 eV – 1.5 eV), high absorption coefficient (>10^4 cm^{-1}) of SnS material which allows SnS to absorb the solar spectrum in an efficient manner [2]. Apart from the above properties, the earth abundance of SnS, low cost and non-toxic nature also considered as important parameters for choosing SnS as a suitable absorber material. SnS and its constituent elements are widely used in different photo-electrochemical cells, energy storage devices, gas sensing elements etc [3]. SnS can be deposited through easy vacuum and non-vacuum based techniques like spray pyrolysis [4], spin coating [5], dip coating [6], sputtering [7], thermal evaporation [8], chemical vapor deposition [9] etc.

Recently, a number of researchers have developed SnS based solar cell practically having ZnS/SnS, ITO/SnS, TiO_2/SnS, CdS/SnS structures [10][11]. The maximum efficiency of SnS based solar cell achieved is 4.36% [12] which is quite low as compared to the solar cell efficiency achieved for CuInGaSe or Cu_2ZnSnS based solar cells. To improve the efficiency of SnS based solar cell, it is very important to understand the device mechanism and its behavior. Theoretical analysis of the solar cell helps us to understand the device mechanism and its behavior in a better manner. Also, in theoretical analysis we can optimize a number of parameters and understand their impact on the solar cell, which is not possible experimentally. So, theoretical analysis in parallel with experimental studies are important to understand the device physics and engineering in depth.

The recombination loss of the photo generated carriers plays a significant role in governing the efficiency of the solar cell. Back contact layer contributes a lot in the recombination process as the contact area is more with the absorber layer of solar cell [13]. Generated and recombined carrier need to be collected at metal contacts to provide power to the load. Surface recombination velocity also plays a critical role in carrier recombination at the back contact. Adding another layer to create an electric field near to the back contact will help to reduce the surface recombination process. To generate the strong electric field, heavily doped semiconductor layer can be added at the rear end to improve the efficiency [14].

Till now, few researchers have studied theoretically the impact of adding a highly doped layer near the back contact of CdTe, CZTS, CZTSe, CIGS, Sb_2S_3 based solar cells [15][16]. The addition of heavily doped layer is showing improved efficiency of solar cell. But impact of the same on SnS based solar cell is not studied till now. In this manuscript, the efficiency of the SnS based solar cell is analyzed thoroughly with the presence of p^+-SnS back surface field layer using SCAPS-1D software. One of the main reason for using p^+-SnS layer is to make a homojunction which will reduce the lattice mismatch among the layers. Different parameters like thickness of the buffer, absorber layer and BSF layer, radiative recombination, defect density, carrier concentration, series and shunt resistance, ambient temperature of operation are optimized and their impact on the performance of solar cell are thoroughly studied. It is found that after optimizing all the parameters the photo conversion efficiency (η) is around 7.22% with an open circuit voltage (V_{oc}) of 359 mV, short circuit current (J_{sc}) of 27 mA/cm^2 and Fill Factor (FF) of 73.5%.

Solar Cell Structure And Material Properties

The schematic diagram of the of the proposed heterojunction solar cell is shown in figure 1. In the structure Ag, ZnO:Al, CdS, SnS, p^+-SnS and Mo were defined as front contact/ transparent conducting oxide, window layer, absorber layer, BSF layer and back contact respectively.

Figure 2 shows the energy band diagram of the Ag/ZnO:Al/CdS/SnS/p^+-SnS/Mo/Glass heterojunction solar cell. It is found from figure 2 that the valance and conduction band of p^+-SnS absorber layer is higher than the SnS absorber layer and the valance band offset (VBO) between them is almost nil. Another added advantage is that the conduction band offset (CBO) between the SnS absorber layer and p^+-SnS BSF layer is suitably high to block the flow of electrons from SnS to back contact which in turn reducing the surface recombination process in the back electrode [17]. By blocking the electrons, BSF layer can improve the J_{sc}, proving as an effective way to improve the solar cell efficiency. After adding the BSF layer, the absorber and BSF layer acts as an absorber layer altogether which improves the absorption of photon and increases the generation of electron-hole pair [18].

Simulation Model

To study the impact of the different parameters on the performance of the solar cell SCAPS-1D software was used to develop the simulation model. Though SCAPS was widely investigated for CZTS, CIGS, CdTe and kesterite thin film solar cell, but the simulation environment of SCAPS can be extended to analyze the performance of solar cell other than the above solar cells. The results extracted from the SCAPS environment containing results of current as well as some more data with detailed analysis. The analysis of SCAPS-1D is based upon Poisson's equation, hole continuity, electron continuity as given below (Benami et al., 2019):

$$\frac{\partial^2\Psi}{\partial x^2}+\frac{q}{\varepsilon}[p(x)-n(x)+N_D-N_A+\rho_p-\rho_n]=0 \quad (1)$$

$$\frac{1}{q}\frac{dJ_p}{dx}=G_{op}(x)-R(x) \quad (2)$$

$$\frac{1}{q}\frac{dJ_n}{dx}=-G_{op}(x)+R(x) \quad (3)$$

Where, ε is known as the dielectric constant, q is termed as electron charge, N_D and N_A are donor and acceptor density respectively, Ψ is electrostatic potential, p, n, are hole and electron concentration, ρ_p, ρ_n, are hole and electron distribution, J_p, J_n are current densities of hole and electron respectively. In the second equation, G_{op} is termed as optical generation rate, R is defined as net recombination from direct and indirect sources. All of above parameters are the function of the position, x.

SCAPS has the capability to represent the recombination profile, steady state band diagram, and transport carrier properties in 1D. SCAPS software gives the GUI to represent the J-V, C-V, Q-V and C-f spectral responses visually.

For the simulation in SCAPS-1D the materials properties are needed to be included in the platform. For the same, the parameter of different layers used in this device structure are extracted from other reported articles. The work function of front and back metal contacts (Ag = 4.73 eV and Mo=5eV) are included in the simulation to obtain the proper device output results. The parameters used for the simulation work are tabulated in Table 1.

Table 1
Materials parameters used for the current simulation [][]

Material Properties	ZnO:Al	SnS	p^+-SnS	CdS
Thickness (nm)	200	Variable	Variable	Variable
Bandgap (eV)	3.3	1.34	1.34	2.4
Electron Affinity (eV)	4.4	4.2	4.2	4.2
Dielectric Permittivity	9	13	13	10
CB Effective Density of State ($1/cm^3$)	2.2×10^{18}	1.8×10^{18}	1.8×10^{18}	2.2×10^{18}
VB Effective Density of State ($1/cm^3$)	1.8×10^{19}	4.76×10^{18}	4.76×10^{18}	1.8×10^{19}
Electron Thermal Velocity (cm/s)	10^7	10^7	10^7	10^7
Hole Thermal Velocity (cm/s)	10^7	10^7	10^7	10^7
Electron Mobility (cm^2/V.s)	10^2	15	15	10^2
Hole Mobility (cm^2/V.s)	25	100	100	25
Donor Density (N_D) (cm^{-3})	10^{20}	0	0	1.1×10^{17}
Acceptor Density (N_A) (cm^{-3})	0	4.76×10^{15}	4.76×10^{18}	0

Result And Discussion

This simulation study was conducted by optimizing the different parameters of the designed solar cell in SCAPS-1D software. First, the buffer, absorber and BSF layer thickness was optimized. To optimize the buffer, absorber and BSF layer thickness, the effect of other parameters like radiative recombination, acceptor density, defect density, series-shunt resistances were taken as null at 300K.

4.1 Impact of variation of thickness of CdS buffer layer

The impact of the thickness of CdS layer on the performance of SnS based thin-film solar cell is analyzed by properly varying the buffer thickness from 50 nm to 120 nm and keeping thickness of other layers constant. Figure 3 showed the impact of thickness variation of CdS layer on the performance of p^+-SnS/SnS based solar cell. It is found that with the variation of CdS layer thickness, the efficiency (η) is almost constant upto 80 nm and then a slight change is observed, as shown in figure 3(a). The short circuit current (J_{sc}) as well as the open circuit voltage (V_{oc}) is showing modification with the change in the buffer layer thickness whereas fill factor (FF) is showing a slight decrease with the increase in the thickness after 80 nm as per figure 3 (b)-(d). So the impact of varying the thickness of buffer layer is negligible on the efficiency of a solar cell having a BSF layer over an absorber layer. The same phenomenon has been observed by some other researchers also [21]. The path covered by the photo-generated carriers to reach the active region increases with the increase in the thickness of buffer layer. With the slight increase in the travel path the recombination increases which in turn reduces the J_{sc} and V_{oc} [22].

4.2 Impact of variation of SnS absorber layer and p^+-SnS BSF layer thickness

The major challenge in the solar cell technology is to fabricate efficient but cost effective solar cell with a thin absorber layer. BSF layer plays a very significant role in reducing the overall thickness of the absorber layer, hence minimizing the cost [18]. To analyze the effect of SnS and p^+-SnS layer on the performance of solar cell, the thickness was varied from 1000 nm to 3000 nm and 200 nm to 1000 nm for SnS and p^+-SnS respectively as shown in figure 4. It is observed that with the increase in the p+ SnS layer thickness, the efficiency (η) is increasing and the highest efficiency (η) is obtained 9.20% for the thickness of SnS ~1800 nm and p^+-SnS~900 nm having all the other parameters like radiative recombination, defect density, series and shunt resistance at zero value. Any further change in the thickness gives a negligible improvement in the efficiency as the recombination of carriers dominates with the increase in the thickness of absorber and BSF layer [23]. The value of short circuit current (J_{sc}) and open circuit voltage (V_{oc}) is also increasing with the increase in the thickness of p^+-SnS whereas for the variation of thickness of SnS the change is almost constant. The maximum J_{sc} and V_{oc} obtained for the device was 29.11 mA/cm^2 and 0.41 volt respectively. The fill factor (FF) is decreasing with the increase in the thickness of the p+ SnS layer [24]. With the increase in the thickness of absorber and BSF layer, more number of carriers is generated with the same amount of incident photon. As reported by other researchers, with the increase in thickness of absorber layer, the spectral response is also improved [25]. Now the amount of material consumption of the absorber layer can be reduced by adding a BSF layer which in turn reduce the back contact recombination and improves the efficiency. Hence with the inclusion of BSF layer helps us to optimize the absorber layer thickness at lower value, thus the overall cost of the solar cell is also optimized [26].

4.3 Impact of variation of radiative recombination coefficient of p^+-SnS/SnS layer

Recombination is one of the most common device phenomenon and majorly responsible in determining the photo conversion efficiency of solar cell. The radiative recombination rate, mainly occurring in direct bandgap semiconductors, should be at its lowest level to get an enhanced efficiency. The value of radiative recombination is mainly dependent on the atomic structure and carrier density of the films which directly affects the V_{oc} of the device [27]. In this work, the radiative recombination coefficient was varied from 10^{-19} cm^3/s to 10^{-1} cm^3/s for both SnS and p+ SnS layer. It is found from figure 5(a) that for both the layers, the optimum range for radiative recombination is in between 10^{-19} cm^3/s to 10^{-9} cm^3/s having efficiency (η) of 8.84%. It is also found that fill factor (FF) is almost constant for the change in the radiative recombination for p^+-SnS as it has very less impact on the same [figure 5(b)]. The short circuit current (J_{sc}) and open circuit voltage (V_{oc}) is showing maximum value in the range between 10^{-19} cm^3/s to 10^{-9} cm^3/s with a value of 28.50 mA/cm^2 and 0.398 volt respectively, [figure 5(c,d)]. With the increase in the recombination rate, the generated carrier collection decreases rapidly. Due to which the V_{oc} reduces [28]. For the above performance analysis, previously obtained optimized results are considered and the defect density, series and shunt resistance were taken as zero.

4.4 Impact of variation of carrier concentration of p^+-SnS/SnS layer

To study the impact of carrier concentration or acceptor density on the performance of solar cell, the concentration was ranged from 10^{10} cm^{-3} to 10^{18} cm^{-3}. It is observed from figure 6(a) that the maximum photo conversion efficiency (η) is obtained for p^+-SnS with a carrier concentration of 10^{18} cm^{-3} whereas the same for SnS can be kept at 10^{16} cm^{-3}. The fill factor (FF), open circuit voltage (V_{oc}) and short circuit current (J_{sc}) are also showing a variation with the change in the carrier concentration of SnS and p^+-SnS as shown in figure 5(b-d). The same analogy was reported by several other researchers [29]. Change in the carrier concentration is responsible to produce the built-in potential at the interface which in turn reduces the recombination and enhances the efficiency upto a certain limit [30]. To determine the effect of carrier concentration, the previously obtained optimized results were taken into consideration.

4.5 Impact of variation of defect density of p^+-SnS/SnS layer

A major parameter influencing the photovoltaic performance of the solar cell is defect density of the layers. With the increase in the defect density, the recombination increases which modifies the efficiency. Hence the value of the defect density needs to be taken care of in a very significant manner [31]. In this work, the value of defect density was varied from 10^{10} cm^{-3} to 10^{18} cm^{-3} to study the impact on the photovoltaic performance of the SnS based solar cell. It is found from figure 7 that the efficiency (η), fill factor (FF), short circuit current (J_{sc}) and open circuit voltage (V_{oc}) is dependent on the defect density of SnS and not of p^+-SnS. Also it is found from figure 7(a) that the maximum efficiency of 7.52% is obtained for the defect density within the range of 10^{10} cm^{-3} to 10^{16} cm^{-3} for SnS. The same type of phenomenon is observed for fill factor (FF), short circuit current (J_{sc}) and open circuit voltage (V_{oc}) also as shown in figure 7 (b-d).

4.6 Impact of the variation of series (R_s) and shunt (R_{sh}) resistance

Series and shunt resistance is a very important parameter to determine the photo conversion efficiency of a solar cell. Mainly the short circuit current (J_{sc}) and open circuit voltage (V_{oc}) is dependent on the series (R_s) and shunt (R_{sh}) resistance []. To study the effect of device resistance on the performance of solar cell, it is varied from 5-10 $\Omega.cm^{-2}$ and 200-2000 $\Omega.cm^{-2}$ for series and shunt resistance respectively. It is observed that maximum efficiency (η) is observed 7.22% for series resistance of 3 $\Omega.cm^{-2}$ and shunt resistance of 1000 $\Omega.cm^{-2}$ [figure 8(a)]. It is also observed that the efficiency (η), fill factor (FF) and short circuit current (J_{sc}) is mainly dependent on the series resistance, R_s and very mild effect is observed with the variation of shunt resistance, R_{sh}, [figure 8(b,c)]. On the other hand, the open circuit voltage (V_{oc}) is totally dependent on shunt resistance, R_{sh} which is increasing with the increase in shunt resistance, R_{sh}.

4.7 Effect of temperature on the performance of solar cell

The working temperature of the solar cell plays an important role on the performance of the cell. As the solar cells are exposed in open environment, the ambient temperature is always a parameter to influence the efficiency of the cell. The relationship between open circuit voltage (V_{oc}), photo current and temperature is given as,

$$V_{oc} = \frac{E_a}{q} - \left(n.\, k_B.\, \frac{T}{q}\right) ln\left(\frac{J_{00}}{J_l}\right)$$

4

where, n is the ideality factor, E_a is activation energy, J_{00} is reverse saturation current, J_l is photo-current, k_B is Boltzmann constant, q is the charge, and T is operating temperature.

To study the effect of the operating temperature on the performance of solar cell, it is varied from 283 K to 323 K. as shown in figure 9. It is found that with the increase in solar cell operating temperature the efficiency (η) decreases along with open circuit voltage (V_{oc}) and fill factor (FF). But the short circuit current (J_{sc}) increases with the increase in operating temperature. With the increase in the temperature different defect states are getting activated and the recombination also get enhanced with the increase in the ambient temperature. This effect reduces the saturation current while increasing the reverse saturation current [[33]]. The carrier concentration, mobility and bandgap get affected by the ambient temperature, which in turn reduces the efficiency with the increase in the temperature. The reverse saturation current increases with the increase in the solar cell temperature which reduces the V_{oc}. With the increase in the temperature, the electrons become excited and the movements of the free carriers get obstructed due to lattice vibrations. Hence the efficiency reduced due to thr collision with the heavily energized electrons [[34]].

Table 2
Optimized device parameter for the p+-SnS/SnS based solar cell.

Optimized Parameter	**SnS**	**p^+-SnS**
Absorber layer and BSF layer thickness	1800 nm	900 nm
Buffer layer thickness	80 nm	
Radiative recombination coefficient	10^{-10} cm^3/s	
Shallow Acceptor density	10^{16} cm^{-3}	10^{18} cm^{-3}
Defect density	10^{15} cm^{-3}	
Series and Shunt Resistance	3 $\Omega.cm^{-2}$ 1000 $\Omega.cm^{-2}$	
Optimized solar cell parameters	η = 7.22%; FF = 73.5%; J_{sc} = 27 mA/cm^2 ; V_{oc} = 0.359 volt	

Table 2 shows the optimized device parameters for p^+-SnS/SnS based solar cell as obtained from this simulation study and Table 3 shows the comparison of efficiency and other device parameters for SnS based solar cell reported in different literature with this simulated work. From the comparison it was found that the maximum efficiency for SnS based solar cell obtained was 5.24%. The reason for having the less efficiency was mainly due to non-uniform junction in between buffer and absorber layer, high series resistance and carrier recombination which in turn reduces the J_{sc} in comparison with conventional CZTS/Se solar cells [35][12]. The previously reported simulated works [41][42] concentrate mainly on the different device parameter of SnS only whereas in our research work we have considered a separate p^+-SnS BSF layer to reduce the back surface recombination which in turn improved the J_{sc}.

Table 3 Comparison of efficiency and device parameters for SnS based solar cell reported in literature compared with this work.

Device Structure	Efficiency (%)	J_{sc} (mA/cm^2)	V_{oc} (V)	FF (%)
Reported experimental work				
TiO_2/n-SnS/SnS/Ag/SnS/p-SnS/ITO (Nguyen et al., 2021) [35]	5.24	17.13	0.450	68
Glass/Mo/SnS/SnO_2/Zn(O,S):N/ZnO/ITO (Sinsermsuksakul et al., 2014) [12]	4.36	20.2	0.372	58
SLG/Mo/SnS/CdS/iZnO/AZO (Yadav et al., 2021) [36]	3.50	18.9	0.334	55.5
SLG/Mo/SnS/CdS/i-ZnO/AZO/Ni/Ag (Cho et al., 2019) [37]	3.05	19.4	0.297	52.8
Glass/Mo/SnS/CdS/i-ZnO/Al:ZnO/Ni/Al (Reddy et al., 2019) [38]	2.28	20.3	0.280	40
SLG/Mo/SnS/CdS/i-ZnO/ZnO:B/Ni/Ag (Kang et al., 2017) [39]	1.61	13.28	0.269	45.07
TCO/CdS/SnS-Cubic/SnS-Orth/Contact (González-Flores et al., 2019) [40]	1.38	6.96	0.488	41
Reported simulated work				
Contact/n-ZnO/n-CdS/p-SnS/Contact (Boubakri et al., 2021) [41]	15.62	33.29	0.752	62.0
Contact/p-SnS/CdS/ZnO/Contact (Ullah et al., 2014) [42]	10.6	13.4	0.920	86.3
Glass/ITO/ZnO/CdS/SnS/Contact (Garain et al., 2021) [20]	8.92	20.75	0.732	36.89
Glass/Mo/SnS/SnO_2/Zn(O,S):N/ZnO/ITO (Minbashi et al., 2018) [44]	7.68	27.99	0.419	67.97
This simulated work				
Ag/ZnO:Al/CdS/SnS/p^+-SnS/Mo/Glass	7.22	27	0.359	73.5

Conclusion

Numerical study to determine the optimized parameters of solar cell helps to determine the insight of different device parameters and its impact on the solar cell. This work was mainly intended to study the impact of variation of thickness of buffer and absorber layer, recombination coefficient, acceptor density, defect density, series-shunt resistance, and operating temperature on the performance of solar cell having back surface field (BSF) layer to reduce the back contact recombination. Research study available on the influence of these parameters of absorber and BSF layer on solar cell performance is very rare. The device structure, Ag/ZnO:Al/CdS/SnS/p^+-SnS/Mo/Glass was simulated using SCAPS-1D software. The reason for using p^+-SnS BSF layer is to create a homojunction which in turn provides a very less lattice mismatch with SnS layer. It was clearly observed from the obtained results that the optimum thickness for CdS, SnS and p^+-SnS is coming 80 nm, 1800 nm and 900 nm respectively. The optimized results shows that by controlling of recombination, acceptor and defect density the efficiency can be improved. Also the series and shunt resistance plays an important role for the device performance. Hence a proper controlling of all these parameters are very important to obtain a highly efficient photovoltaic device having efficiency of 7.22% with FF, J_{sc} and V_{oc} of 73.5%, 27 mA/cm^2 and 0.359 volt respectively. This numerical modelling and analysis of the SnS-based solar cell having p^+-SnS as a BSF layer will help the researchers to develop an solar cell with high efficiency based on non-toxic, earth abundant SnS material.

Declarations

Acknowledgement

All the authors like to thank all the developers of SCAPS-1D from University of Gent to make their software available free of cost. The authors like to acknowledge DST-SERB for their financial support under the grant no. EMR/2017/002196.

Compliance with ethical standards

Conflict of interest: The authors declare that they have no known competing financial interests or personal relationships that could have appeared to influence the work reported in this paper.

References

1. Samy Almosni, Amaury Delamarre, Zacharie Jehl, Daniel Suchet, Ludmila Cojocaru, Maxime Giteau, Benoit Behaghel, Anatole Julian, Camille Ibrahim, Léa Tatry, Haibin Wang, Takaya Kubo, Satoshi Uchida, Hiroshi Segawa, Naoya Miyashita, Ryo Tamaki, Yasushi Shoji, Katsuhisa Yoshida, Nazmul Ahsan, Kentaro Watanabe, Tomoyuki Inoue, Masakazu Sugiyama, Yoshiaki Nakano, Tomofumi Hamamura, Thierry Toupance, Céline Olivier, Sylvain Chambon, Laurence Vignau, Camille Geffroy, Eric Cloutet, Georges Hadziioannou, Nicolas Cavassilas, Pierre Rale, Andrea Cattoni, Stéphane Collin, François Gibelli, Myriam Paire, Laurent Lombez, Damien Aureau, Muriel Bouttemy, Arnaud Etcheberry, Yoshitaka Okada & Jean-François Guillemoles, Material challenges for solar cells in the twenty-first century: directions in emerging technologies, Science and Technology of Advanced Materials, 19(1) (2018) 336-369, DOI: 10.1080/14686996.2018.1433439
2. Dong, Y., Cai, G., Zhang, Q., Wang, H., Sun, Z., Wang, H., Wang, Y. and Xue, S., 2018. Solution-phase deposition of SnS thin films via thermo-reduction of SnS 2. Chemical Communications, 54(16), pp.1992-1995.
3. Gedi, S., Minnam Reddy, V.R., Kotte, T.R.R., Park, C. and Kim, W.K., 2021. Fundamental Aspects and Comprehensive Review on Physical Properties of Chemically Grown Tin-Based Binary Sulfides.

Nanomaterials, 11(8), p.1955.

4. Reddy, K.R., Reddy, P.P., Miles, R.W. and Datta, P.K., 2001. Investigations on SnS films deposited by spray pyrolysis. Optical materials, 17(1-2), pp.295-298.
5. Garmim, T., Chahib, S., Soussi, L., Mghaiouini, R., El Jouad, Z., Louardi, A., Karzazi, O., El Jouad, M., Hlil, E.K., Hartiti, B. and Monkade, M., 2020. Optical, electrical and electronic properties of SnS thin films deposited by sol gel spin coating technique for photovoltaic applications. Journal of Materials Science: Materials in Electronics, 31(23), pp.20730-20741.
6. Chaki, S.H., Chaudhary, M.D. and Deshpande, M.P., 2016. SnS thin films deposited by chemical bath deposition, dip coating and SILAR techniques. Journal of Semiconductors, 37(5), p.053001.
7. Zhao, L., Di, Y., Yan, C., Liu, F., Cheng, Z., Jiang, L., Hao, X., Lai, Y. and Li, J., 2016. In situ growth of SnS absorbing layer by reactive sputtering for thin film solar cells. RSC advances, 6(5), pp.4108-4115.
8. Miles, R.W., Ogah, O.E., Zoppi, G. and Forbes, I., 2009. Thermally evaporated thin films of SnS for application in solar cell devices. Thin Solid Films, 517(17), pp.4702-4705.
9. Ahmet, I.Y., Guc, M., Sánchez, Y., Neuschitzer, M., Izquierdo-Roca, V., Saucedo, E. and Johnson, A.L., 2019. Evaluation of AA-CVD deposited phase pure polymorphs of SnS for thin films solar cells. RSC advances, 9(26), pp.14899-14909.
10. Islam, M.S., Islam, N., Anis-Uz-Zaman, M., Baul, A., Mostafa, S.M.G. and Sreelekha, M., 2019, February. Investigation for Optimal Structure of CdS/SnS Solar Cell from Numerical Analysis. In 2019 International Conference on Intelligent Sustainable Systems (ICISS) (pp. 447-450). IEEE.
11. Kuddus, A., Mostaque, S.K. and Hossain, J., 2021. Simulating the performance of a high-efficiency SnS-based dual-heterojunction thin film solar cell. Optical Materials Express, 11(11), pp.3812-3826.
12. Sinsermsuksakul, P., Sun, L., Lee, S.W., Park, H.H., Kim, S.B., Yang, C. and Gordon, R.G., 2014. Overcoming efficiency limitations of SnS-based solar cells. Advanced Energy Materials, 4(15), p.1400496
13. Zhang, Z., Yao, L., Zhang, Y., Ao, J., Bi, J., Gao, S., Gao, Q., Jeng, M.J., Sun, G., Zhou, Z. and He, Q., 2018. Modified back contact interface of CZTSe thin film solar cells: elimination of double layer distribution in absorber layer. Advanced Science, 5(2), p.1700645.
14. Park, S., Chen, H., Hiura, S., Takayama, J., Sueoka, K. and Murayama, A., 2021. Electric-Field-Effect Spin Switching with an Enhanced Number of Highly Polarized Electron and Photon Spins Using p-Doped Semiconductor Quantum Dots. ACS omega, 6(12), pp.8561-8569.
15. Kc, D., Shah, D.K., Akhtar, M.S., Park, M., Kim, C.Y., Yang, O. and Pant, B., 2021. Numerical Investigation of Graphene as a Back Surface Field Layer on the Performance of Cadmium Telluride Solar Cell. Molecules, 26(11), p.3275.
16. Al Ahmed, S.R., Sunny, A. and Rahman, S., 2021. Performance enhancement of Sb_2Se_3 solar cell using a back surface field layer: A numerical simulation approach. Solar Energy Materials and Solar Cells, 221, p.110919.

17. M. Atowar Rahman, Enhancing the photovoltaic performance of Cd-free Cu_2ZnSnS_4 heterojunction solar cells using SnS HTL and TiO2 ETL, Sol. Energy, 215 (2021), pp. 64-76, 10.1016/j.solener.2020.12.020
18. S.R.I. Biplab, M.H. Ali, M.M.A. Moon, M.F. Pervez, M.F. Rahman, J. Hossain, Performance enhancement of CIGS-based solar cells by incorporating an ultrathin BaSi2 BSF layer, J. Comput. Electron., 19 (2020), pp. 342-352, 10.1007/s10825-019-01433-0
19. Basak, A. and Singh, U.P., 2021. Numerical modelling and analysis of earth abundant Sb_2S_3 and Sb_2Se_3 based solar cells using SCAPS-1D. Solar Energy Materials and Solar Cells, 230, p.111184.
20. Garain, R., Basak, A. and Singh, U.P., 2021. Study of thickness and temperature dependence on the performance of SnS based solar cell by SCAPS-1D. Materials Today: Proceedings, 39, pp.1833-1837.
21. Virang Shukla, Gopal Panda, Effect of BSF layer on the perf*o*rmance of CdTe solar cell,Materials Today: Proceedings, 44(1) (2021) 2300-2303. https://doi.org/10.1016/j.matpr.2020.12.394.
22. A. Bouarissa, A. Gueddim, N. Bouarissa, H. Maghraoui-Meherezi, Modeling of ZnO/MoS_2/CZTS photovoltaic solar cell through window, buffer and absorber layers optimization, Mater. Sci. Eng., B, 263 (2021) 114816, 10.1016/j.mseb.2020.114816
23. Y.S. Lee, T. Gershon, O. Gunawan, T.K. Todorov, T. Gokmen, Y. Virgus, S. Guha, $Cu_2ZnSnSe_4$ thin-film solar cells by thermal co-evaporation with 11.6% efficiency and improved minority carrier diffusion length, Adv. Energy Mater., 5 (2015), pp. 2-5, 10.1002/aenm.201401372
24. Kuddus, A., Mostaque, S.K. and Hossain, J., 2021. Simulating the performance of a high-efficiency SnS-based dual-heterojunction thin film solar cell. Optical Materials Express, 11(11), pp.3812-3826.
25. A.D. Adewoyin, M.A. Olopade, M. Chendo, Enhancement of the conversion efficiency of Cu_2ZnSnS_4 thin film solar cell through the optimization of some device parameters, Optik, 133 (2017), pp. 122-131, 10.1016/j.ijleo.2017.01.008
26. Md. Sohel Rana, Md. Mazharul Islam, M. Julkarnain, Enhancement in efficiency of CZTS solar cell by using CZTSe BSF layer, Solar Energy, 226 (2021) 272-287. https://doi.org/10.1016/j.solener.2021.08.035.
27. Kumar, A. and Thakur, A.D., 2018, September. Improvement of efficiency in CZTSSe solar cell by using back surface field. In IOP Conference Series: Materials Science and Engineering (Vol. 360, No. 1, p. 012027). IOP Publishing.
28. O.K. Simya, A. Mahaboobbatcha, K. Balachander, A comparative study on the performance of Kesterite based thin film solar cells using SCAPS simulation program, Superlattices Microstruct., 82 (2015), pp. 248-261, 10.1016/j.spmi.2015.02.020
29. M.M.A. Moon, M.H. Ali, M.F. Rahman, J. Hossain, A.B.M. Ismail, Design and Simulation of $FeSi_2$-Based Novel Heterojunction Solar Cells for Harnessing Visible and Near-Infrared Light. physica status solidi, a) 217 (2020), p. 1900921, 10.1002/pssa.201900921
30. Shao, S. and Loi, M.A., 2020. The role of the interfaces in perovskite solar cells. Advanced Materials Interfaces, 7(1), p.1901469.

31. Minbashi, M., Ghobadi, A., Yazdani, E., Kordbacheh, A.A. and Hajjiah, A., 2020. Efficiency enhancement of CZTSSe solar cells via screening the absorber layer by examining of different possible defects. Scientific Reports, 10(1), pp.1-14.
32. Dalapati, G.K., Zhuk, S., Masudy-Panah, S., Kushwaha, A., Seng, H.L., Chellappan, V., Suresh, V., Su, Z., Batabyal, S.K., Tan, C.C. and Guchhait, A., 2017. Impact of molybdenum out diffusion and interface quality on the performance of sputter grown CZTS based solar cells. Scientific reports, 7(1), pp.1-12.
33. Wu, L., Ji, Y., Ouyang, B., Li, Z. and Yang, Y., 2021. Low-Temperature Induced Enhancement of Photoelectric Performance in Semiconducting Nanomaterials. Nanomaterials, 11(5), p.1131.
34. Weng, Q., Yang, L., An, Z., Chen, P., Tzalenchuk, A., Lu, W. and Komiyama, S., 2021. Quasiadiabatic electron transport in room temperature nanoelectronic devices induced by hot-phonon bottleneck. Nature Communications, 12(1), pp.1-8.
35. Dai Nguyen, T., Hung, N.M., Arepalli, V.K., Kim, J., Raj, M. and Nguyen, T.T.O., 2021. Synthesis of Ag-embedded SnS films by the RF method for photovoltaic applications. Surfaces and Interfaces, p.101151.
36. Yadav, R.K., Pawar, P.S., Neerugatti, K.E., Nandi, R., Cho, J.Y. and Heo, J., 2021. Effect of intrinsic ZnO thickness on the performance of SnS/CdS-based thin-film solar cells. Current Applied Physics, 31, pp.232-238.
37. Cho, J.Y., Sinha, S., Gang, M.G. and Heo, J., 2019. Controlled thickness of a chemical-bath-deposited CdS buffer layer for a SnS thin film solar cell with more than 3% efficiency. Journal of Alloys and Compounds, 796, pp.160-166.
38. Reddy, V.R.M., Cho, H., Gedi, S., Reddy, K.R., Kim, W.K. and Park, C., 2019. Effect of sulfurization temperature on the efficiency of SnS solar cells fabricated by sulfurization of sputtered tin precursor layers using effusion cell evaporation. Journal of Alloys and Compounds, 806, pp.410-417.
39. Kang, J.Y., Kwon, S.M., Yang, S.H., Cha, J.H., Bae, J.A. and Jeon, C.W., 2017. Control of the microstructure of SnS photovoltaic absorber using a seed layer and its impact on the solar cell performance. Journal of Alloys and Compounds, 711, pp.294-299.
40. González-Flores, V.E., Mohan, R.N., Ballinas-Morales, R., Nair, M.T.S. and Nair, P.K., 2019. Thin film solar cells of chemically deposited SnS of cubic and orthorhombic structures. Thin Solid Films, 672, pp.62-65.
41. A. Boubakri, A. Jouidri, Y. Koumya, A. Rajira, A. Almaggoussi, A. Abounadi, An output characteristics simulation of SnS based solar cells, Materials Today: Proceedings, 2021, ISSN 2214-7853, https://doi.org/10.1016/j.matpr.2021.07.428.
42. Ullah, H. and Mari, B., 2014. Numerical analysis of SnS based polycrystalline solar cells. Superlattices and Microstructures, 72, pp.148-155.
43. M. Minbashi, A. Ghobadi, M.H. Ehsani, H. Rezagholipour Dizaji, N. Memarian, Simulation of high efficiency SnS-based solar cells with SCAPS, Solar Energy, 176 (2018) 520-525. https://doi.org/10.1016/j.solener.2018.10.058.

Figures

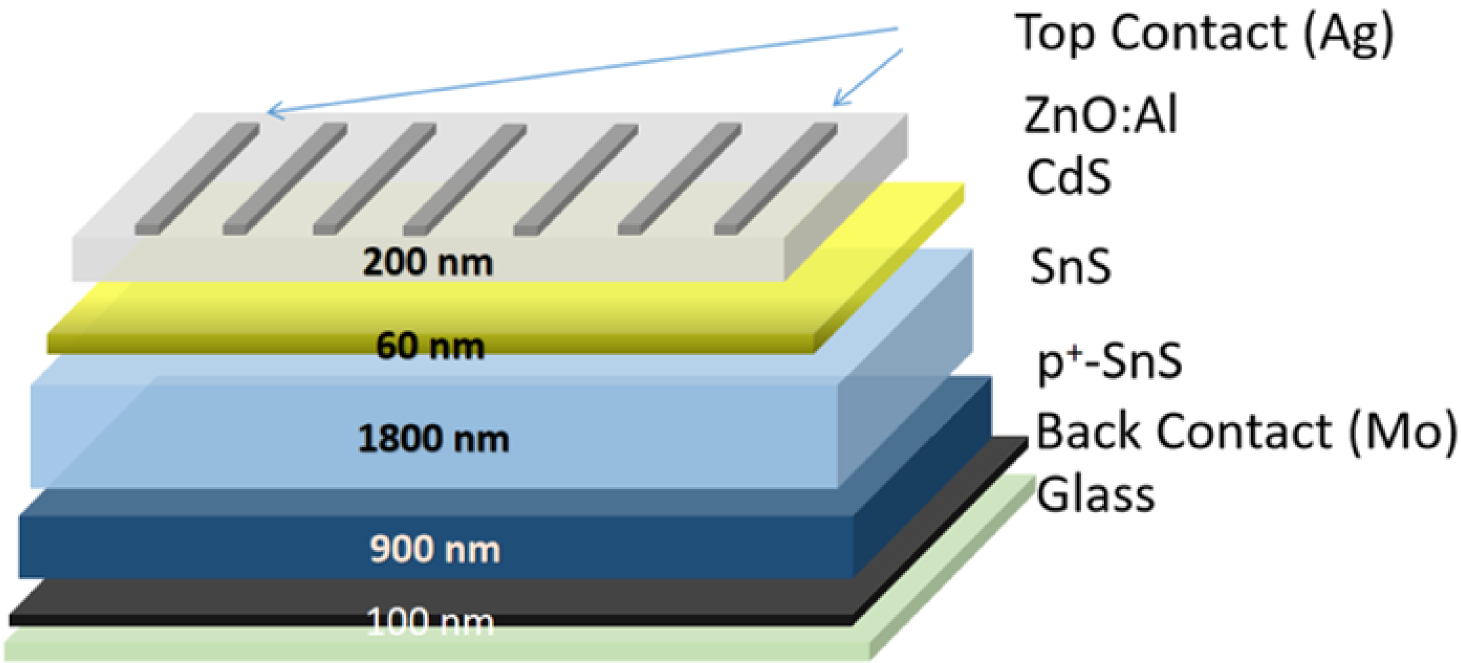

Figure 1

Schematic structure of the simulated device.

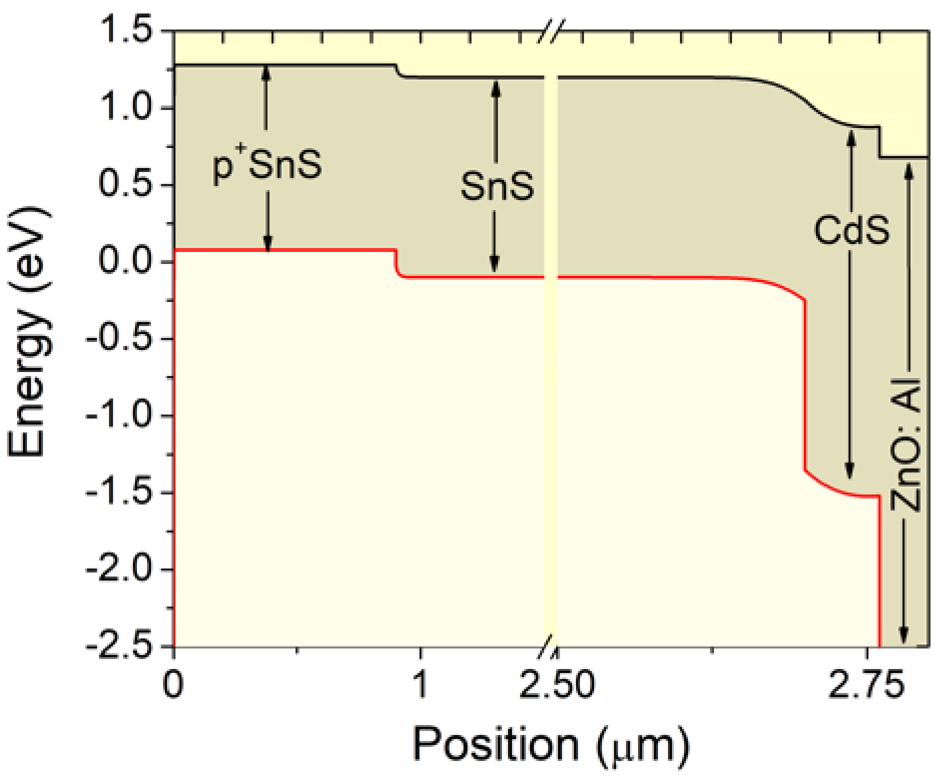

Figure 2

Energy band diagram of the simulated device.

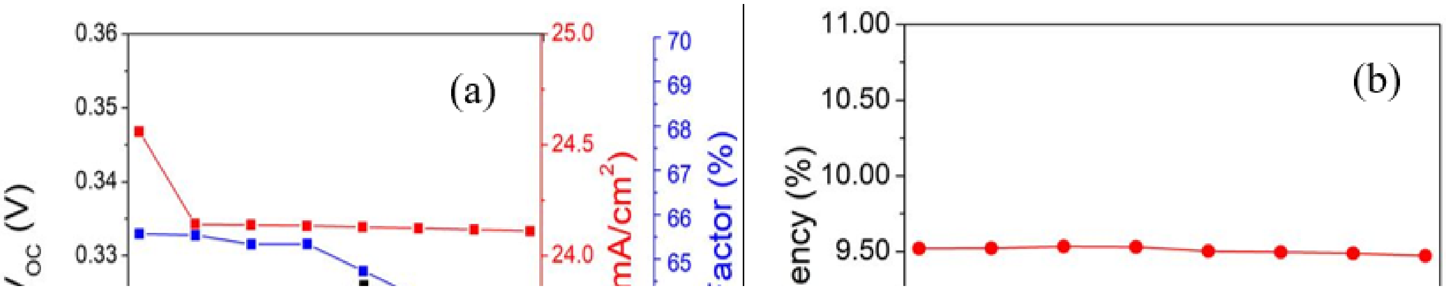

Figure 3

Effect of variation of thickness of buffer layer on the performance of SnS based solar cell.

Figure 4

Effect of variation of thickness of absorber and BSF layer on the performance of SnS based solar cell.

Figure 5

Effect of variation of radiative recombination on different parameters of SnS based solar cell.

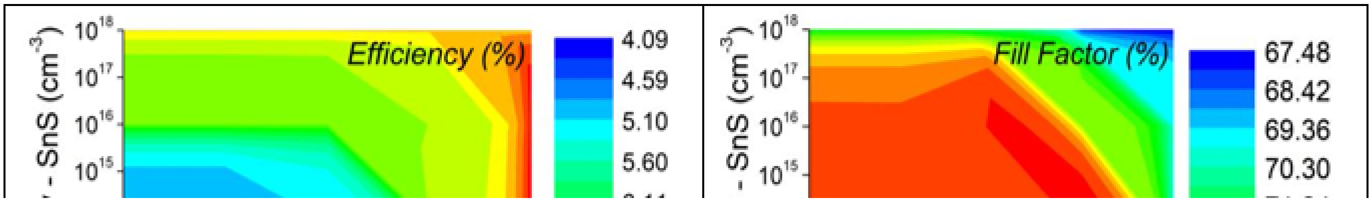

Figure 6

Effect of variation of carrier concentration on the performance of SnS based solar cell.

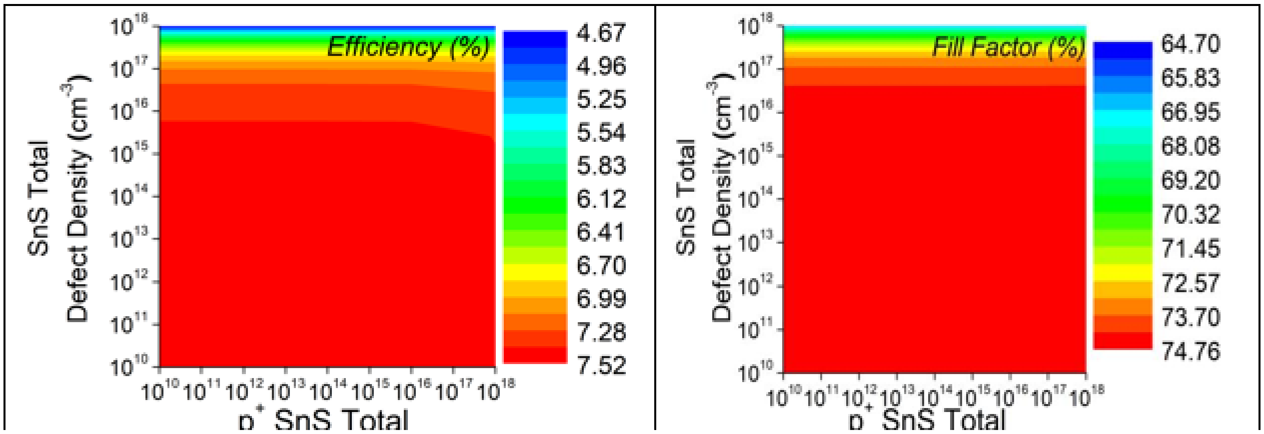

Figure 7

Effect of variation of defect density on the performance of SnS based solar cell.

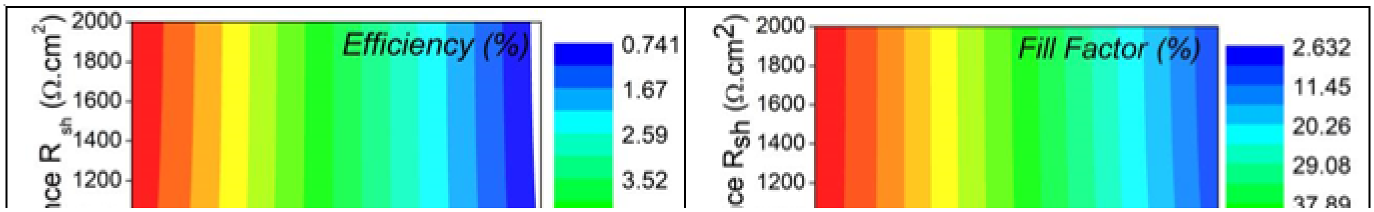

Figure 8

Effect of variation of series (R_s) and shunt (R_{sh}) resistance on the performance of SnS based solar cell.

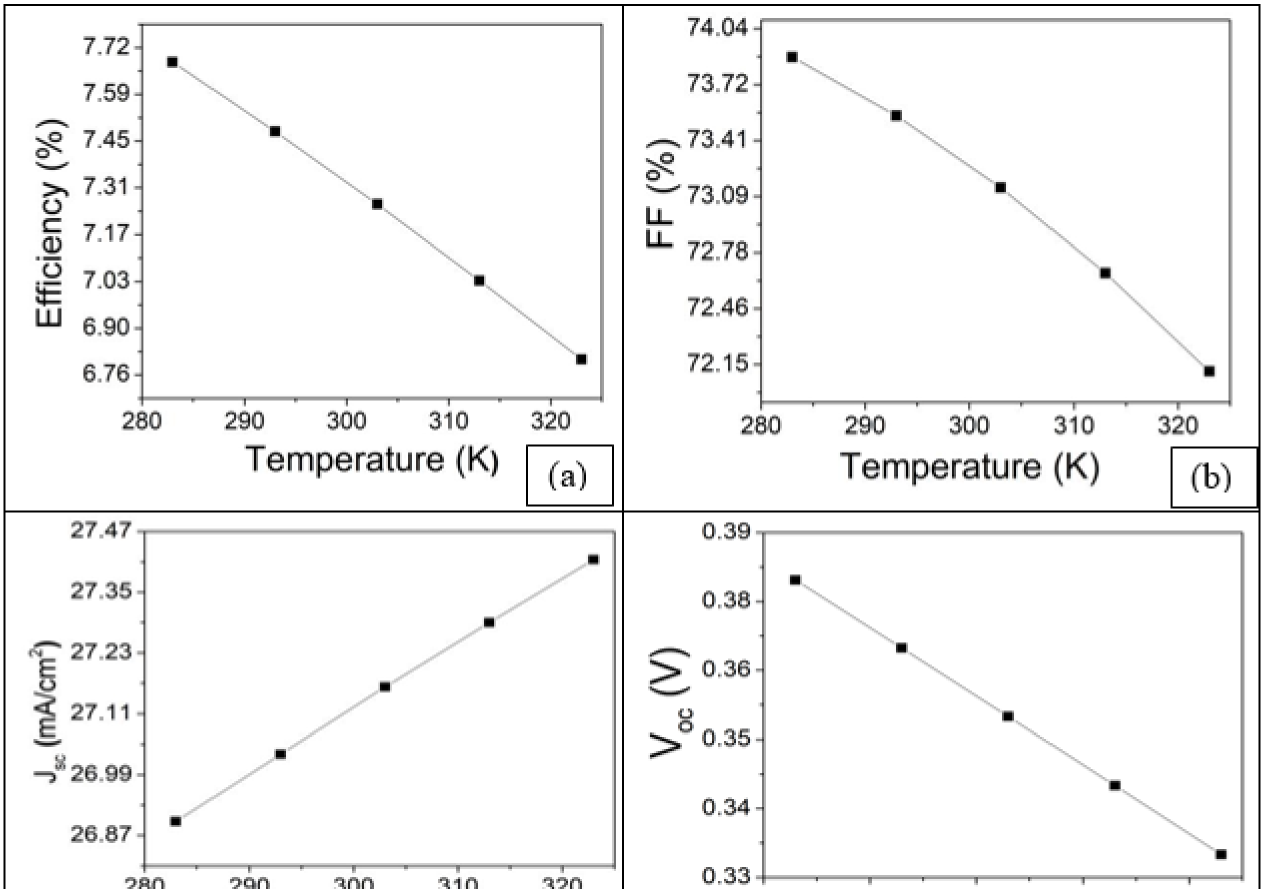

Figure 9

Effect of operating temperature on the performance of SnS based solar cell.